Seismic inversion and the importance of low frequencies

Kris Innanen and Gary Margrave

ABSTRACT

CREWES has made a significant effort this year to support seismic inversion by generating (1) data rich in low frequencies (the Hussar experiment), and (2) model-based methods to extend the spectra of bandlimited data. Here we provide in a tutorial setting illustrations of the reasons why missing low frequencies have such a deleterious influence on inversion. After a brief review of inverse scattering and full waveform inversion, 1D examples quickly expose the influence of low frequencies, as does an example synthesized from Hussar well-log data.

INTRODUCTION

In September of this year, CREWES undertook a broadband seismic experiment near Hussar, Alberta (see Margrave et al., 2011). The primary goal of the experiment was to support seismic inversion by providing data rich in low frequencies. Our purpose in this paper is to present in a tutorial style some of the main reasons why low frequencies are needed in inversion. The reasons are technical, but nevertheless quite accessible, and we can expose them with very simple 1D scalar analytical and numerical examples.

REVIEW

Here we review some of the quantities used in inversion. If you want to get straight to the results, this section can be skipped.

Waves and models

All seismic inversion methods involve (1) a background (or reference) medium, within which we know how waves propagate, and (2) a perturbation, which expresses the difference between this reference and the actual Earth beneath our feet. We begin with wave equations. In 1D, let the scalar wave equation that describes how waves actually propagate in the Earth be

$$\underbrace{\left[\frac{d^2}{dz^2}+\frac{\omega^2}{c^2(z)}\right]}_{\text{actual wave operator}}\underbrace{P(z,z_s,\omega)}_{\text{wave field in Earth}}=\underbrace{\delta(z-z_s)}_{\text{source}}. \tag{1}$$

It has three main parts: (1) a wave operator, which contains the properties of the medium; (2) the wave field P which propagates in the medium; and (3) a source term, which we will take to be a simple impulse located at z_s. Next, consider a "modeling" wave equation, with the right physics but with a reference medium, $c_0(z)$, that is distinct from $c(z)$:

$$\underbrace{\left[\frac{d^2}{dz^2}+\frac{\omega^2}{c_0^2(z)}\right]}_{\text{background medium}}\underbrace{G(z,z_s,\omega)}_{\text{modelled wave field}}=\delta(z-z_s). \tag{2}$$

In the seismic inverse problem, an initial medium $c_0(z)$ is adjusted to be as close as possible to $c(z)$, through use of measurements of P.

Two approaches to this inverse problem have attained real stature in exploration seismology: inverse scattering and full waveform inversion. They are very different, but one thing they have in common is that they both involve a breakup of the actual medium, $c(z)$, into a part that agrees with the reference medium, and a difference term. We define $s(z)$, or the "model", the unknown in the seismic inverse problem, as follows:

$$s(z) = \frac{1}{c^2(z)} = \underbrace{\frac{1}{c_0^2(z)}[1 - \alpha(z)]}_{\text{inverse scattering}} = \frac{1}{c_0^2(z)} - \frac{\alpha(z)}{c_0^2(z)} = \underbrace{s_0(z) + \delta s(z)}_{\text{full waveform inversion}} . \tag{3}$$

Two slightly different ways of breaking up the model are shown. One appears explicitly in terms of the reference scalar wavespeed model $c_0(z)$, and a dimensionless perturbation $\alpha(z)$. This breakup is typical of inverse scattering. The other makes use of the s notation, and involves a reference $s_0(z)$ and a difference term $\delta s(z)$ in the same units. This breakup is typical of full waveform inversion.

The final quantity we wish to introduce at this stage is an exact, analytic form for the modeled Green's function G, which holds for a homogeneous scalar wavespeed c_0:

$$G(z, z_s, \omega) = \frac{e^{ik|z-z_s|}}{i2k} \tag{4}$$

where $k = \omega/c_0$, though any $k_n = \omega/c_n$ might be used.

Inverse scattering

The goal in inverse scattering is to develop formulas by which the perturbation α is directly calculated from measurements of P, given $c_0(z)$ and G. From PDE theory, if we know the Green's function for a wave operator like $[\cdot]$ in equation (2), then determining the field for a more complicated source is easy: we multiply the source by the Green's function and integrate. We can use this trick to solve for P. Using equation (3), we replace $c(z)$ in equation (1) with c_0 and α, and then bring the α term to the right hand side:

$$\left[\frac{d^2}{dz^2} + k_0^2(z)\right] P(z, z_s, \omega) = \delta(z - z_s) + k_0^2(z)\alpha(z)P(z, z_s, \omega). \tag{5}$$

This is exactly what we need — a wave operator like the one in equation (2) and a more complicated source. P is determined now by multiplying it by G and integrating:

$$P(z, z_s, \omega) = G(z, z_s, \omega) + \int dz' G(z, z', \omega)k_0^2(z)\alpha(z')P(z', z_s, \omega). \tag{6}$$

We haven't solved for P yet, since it is also under the integral on the right. But, this P can be replaced by the *whole* right hand side, since the whole right hand side also equals P.

Doing this an infinite number of times we create the Born series

$$\begin{aligned}P(z,z_s,\omega) = G(z,z_s,\omega) &+ \int dz' G(z,z',\omega) k_0^2(z')\alpha(z')G(z',z_s,\omega) \\ &+ \int dz' G(z,z',\omega)k_0^2(z')\alpha(z') \int dz'' G(z',z'',\omega)k_0^2(z'')\alpha(z'')G(z'',z_s,\omega) \\ &+ \ldots \quad .\end{aligned} \tag{7}$$

If we subtract G from both sides, and fix z and z_s to be on some measurement surface, equation (7) becomes a model for our data $D(\omega) = P - G|_{\text{measured}}$. It can be directly inverted as follows. We form the inverse series $\alpha(z) = \alpha_1(z) + \alpha_2(z) + \ldots$, in which α_n is defined to be nth order in measurements of $D(\omega)$, and equate like orders. This produces a sequence of equations:

$$\begin{aligned}D_1(\omega) &= \int dz' G(z,z',\omega)k_0^2(z')\alpha_1(z')G(z',z_s,\omega), \\ D_2(\omega) &= \int dz' G(z,z',\omega)k_0^2(z')\alpha_2(z')G(z',z_s,\omega), \\ &\vdots\end{aligned} \tag{8}$$

etc., where $D_1 = D(\omega)$,

$$D_2 = -\int dz' G(z,z',\omega)k_0^2(z')\alpha_1(z') \int dz'' G(z',z'',\omega)k_0^2(z'')\alpha_1(z'')G(z'',z_s,\omega), \tag{9}$$

and so on, with the D_n becoming progressively more complicated functions of lower order D's as n grows. We can solve the first equation in (8) for $\alpha_1(z)$, use $\alpha_1(z)$ to make D_2 using equation (9), put that into the second equation in (8), solve for $\alpha_2(z)$, and continue this process. Summing these up we eventually reconstruct the full $\alpha(z)$.

It has been recognized (Clayton and Stolt, 1981) that, at any stage in equation (8), something akin to migration is going on. Solving

$$D_1(\omega) = \int dz' G(z,z',\omega)k_0^2(z')\alpha_1(z')G(z',z_s,\omega) \tag{10}$$

for $\alpha_1(z)$, for instance, involves inverting the operator $\int G[\cdot]G$. The right G acts from left to right, bringing the wave from the model point z' at depth to the source z_s. The left G acts from right to left, bringing the wave from the model point z' to the receiver z. Stripping these off, to expose α_1, undoes these two operations, effectively downward continuing sources and receivers and applying an imaging condition simultaneously.

Full waveform inversion

We next go back to the start again and discuss the basic form for full waveform inversion, an iterative methodology in which modeled and measured fields are compared and the former is updated. Recall we discuss two fields, P and G; here they signify

$$\begin{aligned}&P(z_g,z_s,\omega): \quad \text{Field in actual medium,} \quad \text{DATA} = P|_{\text{ms}} \\ &G(z_g,z_s,\omega|s_0^{(n)}): \quad \text{Modeled field in current medium model iteration } s_0^{(n)}.\end{aligned} \tag{11}$$

To compare them at a particular iteration, we take their difference to be δP:

$$\delta P(z_g, z_s, \omega | s_0^{(n)}) \equiv P(z_g, z_s, \omega) - G(z_g, z_s, \omega | s_0^{(n)}). \tag{12}$$

The model is the wavespeed structure of the medium with which we calculate G. We discuss it in terms of s_0. Our aim will be to take a *current* version of s_0, and, by analyzing the measured data, *update* it so that it after the update it is closer to the actual medium than it was before. For our current purposes we envision the step:

$$s_0^{(n+1)}(z) = s_0^{(n)}(z) + \mu^{(n)} g^{(n)}(z), \tag{13}$$

where μ is the step-length, and g is the “direction” of the step.

To discuss the direction g, we choose an objective-function which is (1) expressed in terms of the medium model and our measured data, and (2) is (by assumption) small when the medium model is close to the actual model, and large when the medium model is far from the actual model. An objective function Φ which fits this bill is just the magnitude of the differences δP:

$$\Phi \equiv \frac{1}{2} \int d\omega \left\{ |\delta P|^2 \right\}. \tag{14}$$

The objective function is usefully thought of as a kind of landscape of hills and valleys, with a point on the landscape for every possible model. Where the model and the actual medium are very different is “higher ground” on the landscape, since Φ has a greater value there. We say that we have solved the inverse problem when we have found the model associated with the lowest point on Φ — the bottom of the deepest valley, where the model and the medium are maximally in agreement.

If a guess s_0 lands us anywhere other than the lowest point on Φ, a good step to take, it would seem, is directly “downhill”: the same direction a ball would roll if we put it on the landscape and let it go. That direction is the gradient of Φ. Let, then, g be the gradient of Φ taken with respect to each model parameter (i.e., $s_0(z)$ at each depth z). Skipping the algebra, taking the derivative of equation (14) with respect to s_0 we get the integral of the product of two terms:

$$g^{(n)}(z) = -\int d\omega \mathrm{Re} \left\{ \frac{\partial G(z_g, z_s, \omega | s_0^{(n)})}{\partial s_0^{(n)}(z)} \delta P^*(z_g, z_s, \omega | s_0^{(n)}) \right\}. \tag{15}$$

By way of terminology, in equation (15) the quantities

$$\frac{\partial G(z_g, z_s, \omega | s_0^{(n)})}{\partial s_0^{(n)}(z)}, \quad \text{and} \quad \delta P(z_g, z_s, \omega | s_0^{(n)}), \tag{16}$$

are referred to as the *sensitivities* (or *Fréchet derivatives*), and the *data residuals* respectively. A final bit of (skipped) algebra and we derive a form for the sensitivities that holds for wave-type problems:

$$\frac{\partial G(z_g, z_s, \omega | s_0^{(n)})}{\partial s_0^{(n)}(z)} = -\omega^2 G(z_g, z, \omega | s_0^{(n)}) G(z, z_s, \omega | s_0^{(n)}), \tag{17}$$

in which case the gradient, or step direction to take away from our initial guess, is

$$g^{(n)}(z) = \int d\omega\omega^2 [G(z, z_s, \omega|s_0^{(n)})] \times [G(z_g, z, \omega|s_0^{(n)})\delta P^*(z_g, z_s, \omega|s_0^{(n)})]. \qquad (18)$$

Remarkably (given how different this derivation is from that of inverse scattering), this step direction, the calculation of which is the engine of full waveform inversion, is also closely related to migration. Evidently, at any given step, we take the residuals δP, time reverse them (via the *), backpropagate them from the receiver z_g to a depth point z, via the $G(z_g, z, \omega|s_0^{(n)})$ term, forward model a source wave field from z_s to the same point z, via the $G(z, z_s, \omega|s_0^{(n)})$ term, and correlate them. This is equivalent to downward continuation of sources and receivers followed by the application of an imaging condition.

Expressing layers and steps mathematically

Later we will choose, as example models, sets of layers where each layer has a particular velocity c. We will write down what reflection data from such a model will look like, choose a simple background medium, and then see how full waveform inversion acts to re-create the layers. This will be a mathematical (but insightful!) exercise. So, to see whether FWI is doing what it should, we will need to be able to recognize the layers when they appear, mathematically, in the results.

We will express layers as sums of functions H which each represent a single step, of a certain height at a certain place. These are called Heaviside functions, and are defined as

$$H(z) = \begin{cases} 0 & z < 0 \\ 1 & z > 0 \end{cases}. \qquad (19)$$

$H(z)$ is the antiderivative of the delta function: $H(z) = \int_{-\infty}^{z} \delta(z')dz'$. So, since the inverse Fourier transform of a delta function centred at z_0 is

$$\delta(z - z_0) = \frac{1}{2\pi}\int dk_z e^{ik_z(z-z_0)}, \qquad (20)$$

by taking the antiderivative of both sides of equation (20), we obtain for the Heaviside function

$$H(z - z_0) = \frac{1}{2\pi}\int dk_z \frac{e^{ik_z(z-z_0)}}{ik_z}. \qquad (21)$$

Recognizing these will help interpreting the full waveform inversion examples to come.

INVERSE SCATTERING I: DATA SPECTRUM AND MODEL SPECTRUM

The easiest way to see how important low frequencies are to inversion, and *where* in the reconstructed model they make their presence known, is to examine the inverse scattering problem in the linear regime. That is, we take the first term in the Born series in equation (8), and, assuming the perturbation to be small, make the approximation $\alpha(z) \approx \alpha_1(z)$, in which case we have the self contained relationship

$$D(\omega) = \int dz' G(z, z', \omega) k_0^2(z')\alpha(z')G(z', z_s, \omega). \qquad (22)$$

Let us next assume a homogeneous reference medium with wavespeed c_0, in which case we may use the Green's function in equation (4). Using the fact that in a reflection experiment z and z_s, the receiver and source depths, are both less than the depth support of the perturbation (i.e., all the unknown structure is below our feet), we have

$$\begin{aligned} D(\omega) &= \int dz' \left[\frac{e^{ik_0(z'-z)}}{i2k_0}\right] k_0^2\alpha(z') \left[\frac{e^{ik_0(z'-z_s)}}{i2k_0}\right] \\ &= \frac{k_0^2}{(i2k_0)^2} e^{-ik_0(z+z_s)} \int dz' e^{i2k_0 z'} \alpha(z') \\ &= A(\omega)\hat{\alpha}\left(-2\frac{\omega}{c_0}\right), \end{aligned} \tag{23}$$

where in the last step we have (1) accumulated all the pre-factors into A, and (2) recognized that the remaining parts of the Green's functions, appearing under the integral, turn the integral into a Fourier transform over depth. The $\hat{\alpha}$ are, then, the Fourier coefficients of α. Inspecting the transform, we see that the factor $-2\omega/c_0$ is the Fourier dual of depth z. Hence, we may refer to it as k_z, the depth wavenumber. We have in other words produced a simple relationship between data and model:

$$D(\omega) \propto \hat{\alpha}\left(k_z\right). \tag{24}$$

The inverse problem now could not be simpler: we take temporal frequencies from our data (D), and populate the spatial frequencies of the model ($\hat{\alpha}$). Once they are full populated, through an inverse Fourier transform we have a reconstruction of $\alpha(z)$.

Also clear is the influence of missing low frequencies. Since $k_z \propto \omega$, a missing low frequency datum will translate to a similar missing low wavenumber datum; hence missing low data frequencies will translate into missing low wavenumber, or smoothly varying, parts of the model.

A further important point (especially for the nonlinear parts of inverse scattering and the higher order iterations of full waveform inversion): models that have been reconstructed without their low wavenumbers lose their ability to sustain structure in depth. A simple numerical example will demonstrate. Suppose data from a two layer model are inverted using equation (24). In Figure 1 the spectrum of these data are plotted three times (top row), each time with more of the low frequency content having been removed. Below the consequent linearized reconstructions $\alpha(z)$ are plotted in black, with the full bandwidth results in blue for comparison.

The models with missing low frequency exhibit a characteristic "droop". Consider the bandlimited reconstruction of the shallowest interface in the bottom right panel. An interface is more or less discernible in the expected location, but the lower medium cannot sustain in depth the step in wavespeed. This problem, which inverse scattering shares equally with full waveform inversion, will be seen to cause issues in nonlinear corrections in the former case, and in iterative updating in the latter case.

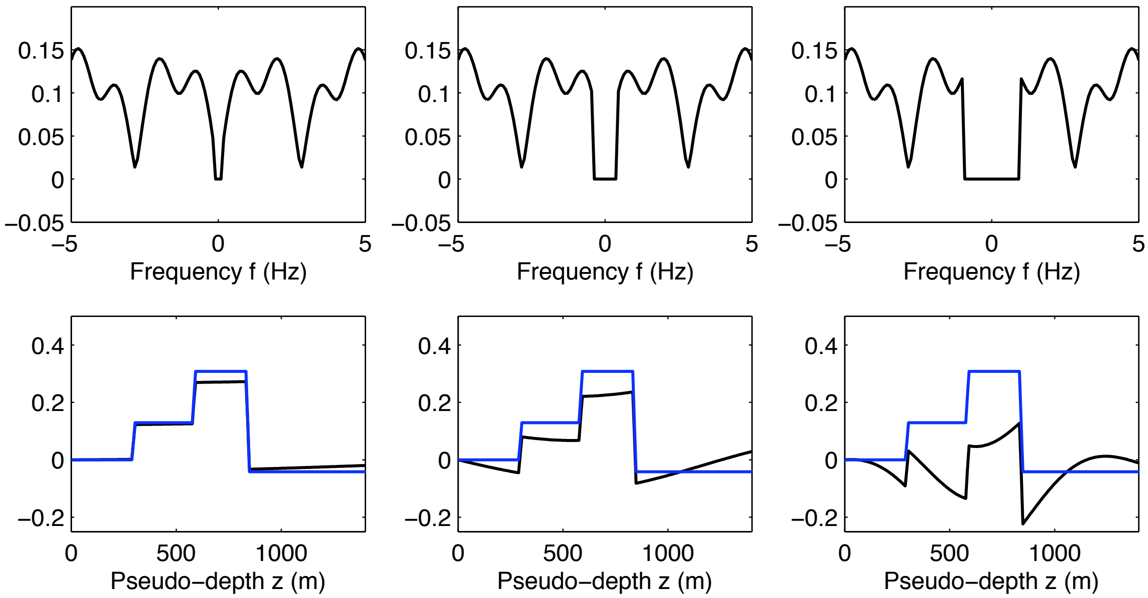

FIG. 1. Linear inverse scattering reconstruction of a two-layer medium with progressive loss of low frequency content. Top row: data spectra; bottom row: linear reconstruction at full bandwidth (blue) and with low frequencies removed (black). Left column: 0 Hz missing; middle colum: 0-0.5 Hz missing; right column: 0-1 Hz missing.

INVERSE SCATTERING II: PROPAGATION THROUGH THE PERTURBATION

In equation (24) and in Figure 1 the importance of low frequencies to linearized inversion is illustrated. Unfortunately, this importance only grows when nonlinear adjustment of the linear approximation is attempted. The correct construction of the data-like quantities D_n in equation (8) turns out to be highly sensitive to bandwidth.

Let us see this by evaluating equation (9), that is, determining D_2 in terms of the linear result $\alpha_1(z)$ pictured in Figure 1, and then inverting the Green's operators to calculate $\alpha_1(z)$. Substituting the homogeneous Green's function in equation (4) into equation (9) and manipulating the result, we obtain

$$\alpha_2(z) = -\frac{1}{2}\frac{d}{dz}\left(\alpha_1(z)\int_0^z dz'\alpha_1(z')\right). \tag{25}$$

Going further, we can select a subset of all the terms in the inverse series α_1, α_2, ..., and sum them, forming the nonlinear inverse approximation

$$\alpha_{NL}(z) \approx \frac{1}{2\pi}\int dk_z \int dz' \exp\left\{-ik_z\left[z' - \frac{1}{2}\int_0^{z'} dz''\alpha_1(z'')\right]\right\}\alpha_1(z'). \tag{26}$$

The new inverse result is, given full bandwidth data, a closer approximation to $\alpha(z)$ than was the linear result (Innanen, 2008).

Equation (26) is a formula which, given a data trace, calculates the medium perturbations $\alpha(z)$ to a high degree of accuracy. How does it respond to missing low frequencies?

Notice that it — like all of the individual terms that make it up —involves the integral of $\alpha_1(z)$, which really means the integral of the data: $\int_0^z dz'\alpha_1(z')$. The purpose of integrating in this way is, essentially, to drive inversion by expressing wave propagation through a medium other than the reference medium — through the perturbation. An analogy is the WKBJ approximation, in which a field has roughly the form

$$\psi \approx \exp\left(i\omega \int_0^z \frac{dz'}{c(z')}\right), \tag{27}$$

wherein the wave is given the correct phase by integrating through the medium $c(z)$.

The integral of the full bandwidth signal (blue) and the bandlimited signal (black) in the bottom right corner of Figure 1, whichever is being used, is the only thing that makes the nonlinear output $\alpha_{NL}(z)$ in equation (26) different from the linear input $\alpha_1(z)$. If $\int_0^z \alpha_1(z')dz' \rightarrow 0$, then the two integrals become nested forward and inverse Fourier transforms, taking α_1 to the Fourier domain and then back again, unchanged. But by eye, zero is exactly what the integral of the bandlimited signal will be. Bandlimitation will render all the nonlinear work we have done irrelevant.

To summarize, for the nonlinear adjustments within inverse scattering to work, requires that the linear reconstruction allow notional waves to be calculated propagating through it. This is not possible with significantly bandlimited data.

FULL WAVEFORM INVERSION I: PROPAGATION THROUGH THE UPDATE

For all their differences, FWI and inverse scattering share in degree and kind this sensitivity to missing low frequencies. Let us see this next.

Full waveform inversion is not inherently analytical in nature, but rather occurs in iterative, usually highly numerical, steps. So, formulas like equation (26) are never determined in FWI, and consequently we don't have the same ability to analyze its behaviour. We will have to work a little harder to gain insight into the problem, by putting analytic data through one FWI iteration, and watching what gets made.

The models we will perform this exercise on are illustrated in Figures 2a–b. In Figure 2a we illustrate a completely homogeneous medium with waves propagating with velocity c_0 everywhere. This will serve as our background, or intial medium. It is the sort of starting model one would be forced to use with no prior knowledge of even the smooth background velocity of the Earth. In Figure 2b is a two-interface medium with three wave velocities c_0, c_1 and c_2. We will pretend that this represents the actual Earth, and we will take a FWI iteration towards reconstructing it, given reflection data and the background medium as ingredients.

In a single iteration of gradient-based FWI, the background model (which is homogeneous in our case) will be adjusted by adding a scalar times the gradient of the objective function. The scalar is generally determined by a line search. Here we will not worry about the absolute scale of the correction, but instead its structure and relative amplitudes. So,

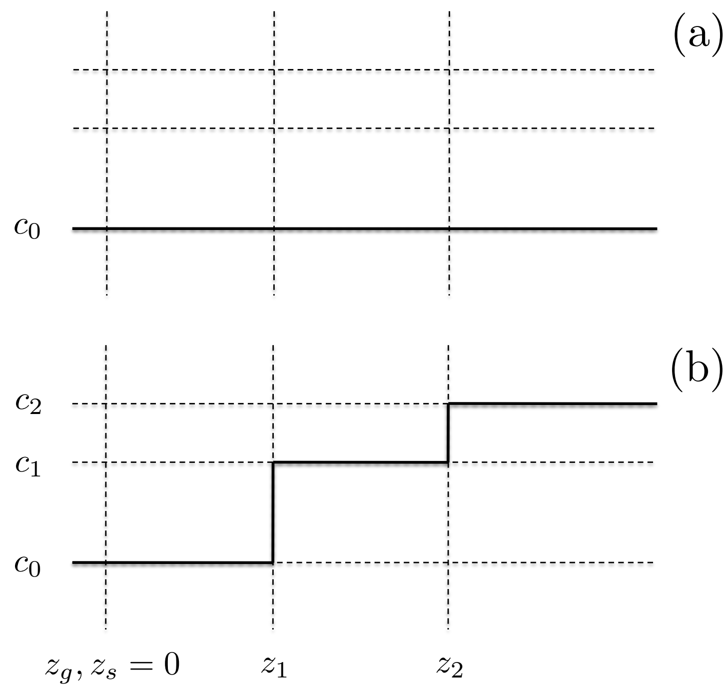

FIG. 2. Models used for analytic calculation of a single FWI iteration. (a) Initial, or background medium, a homogeneous wholespace with velocity c_0; (b) The "actual" medium, consisting of two reflectors.

we can focus on the gradient alone. From equation (18) we have its form:

$$g(z) = \int d\omega \omega^2 [G(z, 0, \omega)] \times [G(0, z, \omega) \delta P^*(0, 0, \omega)]. \tag{28}$$

To calculate g for one step, we evidently need to calculate three things: two modelling Green's functions for each point z in the medium, and the residuals, which are the differences between the data and the modelled field for the fixed source and receiver point, which we will take to be $z_g = z_s = 0$.

The data in the "actual" medium (absent multiples) include the direct wave, $G(0, 0, \omega) = (i2k_0)^{-1}$, and reflections from the boundaries at depths z_1 and z_2. In the frequency domain the data have the analytic form

$$D(\omega) = \frac{1}{i2k_0} + R_1 \frac{e^{i2k_0 z_1}}{i2k_0} + R_2' \frac{e^{i2k_0 z_1}}{i2k_0} e^{i2k_1(z_2 - z_1)}, \tag{29}$$

where the two wavenumbers are $k_0 = \omega/c_0$, $k_1 = \omega/c_1$, and the two amplitudes are $R_1 = (c_1 - c_0)/(c_1 + c_0)$, $R_2' = (1 - R_1^2) R_2$, and $R_2 = (c_2 - c_1)/(c_2 + c_1)$. So, the complex conjugate of the residuals is

$$\begin{aligned} \delta P^*(0, 0, \omega) &= [D(\omega) - G(0, 0, \omega)]^* \\ &= \left[\frac{1}{i2k_0} + R_1 \frac{e^{i2k_0 z_1}}{i2k_0} + R_2' \frac{e^{i2k_0 z_1}}{i2k_0} e^{i2k_1(z_2 - z_1)} - \frac{1}{i2k_0} \right]^* \\ &= -R_1 \frac{e^{-i2k_0 z_1}}{i2k_0} - R_2' \frac{e^{-i2k_0 z_1}}{i2k_0} e^{-i2k_1(z_2 - z_1)}. \end{aligned} \tag{30}$$

Since the two modelled fields are

$$G(z, 0, \omega) = G(0, z, \omega) = \frac{e^{ik_0 z}}{i2k_0}, \tag{31}$$

the fully assembled gradient is given by

$$\begin{aligned} g(z) &= -\int d\omega\omega^2 \frac{e^{i2k_0 z}}{(i2k_0)^2}\left[R_1 \frac{e^{-i2k_0 z_1}}{i2k_0} + R_2' \frac{e^{-i2k_0 z_1}}{i2k_0} e^{-i2k_1(z_2 - z_1)}\right] \\ &= \frac{R_1 c_0^2}{4}\int d\omega \frac{e^{i2k_0(z-z_1)}}{i2k_0} + \frac{R_2' c_0^2}{4}\int d\omega \frac{e^{i2k_0(z-Z_2)}}{i2k_0}, \end{aligned} \tag{32}$$

where

$$Z_2 = z_1 + \frac{k_1}{k_0}(z_2 - z_1). \tag{33}$$

To evaluate the two integrals, we replace $d\omega$ with

$$d\omega = \frac{c_0}{2} \times d(2k_0), \tag{34}$$

such that

$$g(z) = \frac{R_1 c_0^3}{8}\int d(2k_0)\frac{e^{i2k_0(z-z_1)}}{i2k_0} + \frac{R_2' c_0^3}{8}\int d(2k_0)\frac{e^{i2k_0(z-Z_2)}}{i2k_0}, \tag{35}$$

which allows us to immediately write

$$g(z) = \frac{R_1 c_0^3 \pi}{4} H(z - z_1) + \frac{R_2' c_0^3 \pi}{4} H(z - Z_2), \tag{36}$$

having recognized the Fourier forms for step functions discussed in equation (21). Again, we will not put too much stock in the significance of the absolute amplitudes at the moment, but consider the relative amplitudes of the parts of g and its spatial structure. We can evidently say that

$$g(z) \propto H(z - z_1) + \frac{R_2'}{R_1} H(z - Z_2), \tag{37}$$

where, using the definitions of the wavenumbers and equation (33),

$$Z_2 = z_1 + \frac{c_0}{c_1}(z_2 - z_1). \tag{38}$$

The first thing to say about what happens when we add the gradient in equation (37) to the reference medium, is that it is a big improvement. We go from a first guess, containing no interfaces, to a second guess, containing the right number of interfaces (i.e., the two steps H, one at z_1 and one at Z_2).

Equally clearly we have not achieved "the right answer". We know that the correct depth of the lower reflector is z_2. We have misplaced it, putting it at $Z_2 \neq z_2$. Also in general the relative amplitude difference R_2'/R_1 is not precisely correct (see Figure 3).

To get at the issue of low frequency, we focus on the location of the lower interface. How wrong is it? By inspection of equation (38), the more c_1 differs from c_0, the more wrong Z_2 is. Indeed, Z_2 would equal z_2 if c_1 was equal to c_0. The size of the placement error, E, is proportional to the ratio $(1 - c_0/c_1)$:

$$E = |Z_2 - z_1| = \left(1 - \frac{c_0}{c_1}\right) |z_1 - z_2|. \tag{39}$$

That makes sense. If the background medium velocity, i.e., our initial guess, was *correct*, all interfaces would be correctly placed—notice, for instance, the interface at z_1 which by chance was overlain by a medium that agrees with the background model, was placed correctly. This particular iteration only has c_0 as a velocity to work with, even on data events whose history includes propagation at velocity c_1, so some level of error was an inevitability.

The next iteration will know more, since the new medium (the one we will model in next time around) is the background plus the update, and the update knows about these new velocities. Well — it knows *more* about them, though it does not know exactly where they start and end, nor their exact value.* If we were to carry out the next iterate, the new modelling fields G would propagate through the update, that is, through the profile in Figure 3b instead of the profile in Figure 2a. The difference between *placed interface* and *actual interface* at the next iterate will contend with an error E whose factor $(\cdot)$ is much closer to zero.

This is where the low frequency issue comes in. Where did these robust steps H pictured in Figure 3 come from? Entirely from the data, via δP. Now, we have seen what a bandlimited step looks like in Figure 1. This, more or less, is what will be added to the homogeneous reference medium if we do not supply low frequencies. The problem is evident. Propagating a wave through the full bandwidth (blue) profile in the bottom right of Figure 1 will better predict the data, and shrink the residuals. Propagating a wave through the bandlimited (black) update, whose integral is zero, has no effect on the accuracy of the predicted data, and is therefore unable to shrink the residuals.

In practice, of course, what one does is supply a background model carrying the low wavenumbers. But, as a local demonstration of what happens when the actual and background media differ, our results still hold. You could imagine the profiles in Figure 3 as being zoomed in portions of a much larger model, in which the background medium contains the grossest features of the actual model correctly, but still differ here in the manner shown. The residuals due to this part of the update are equivalently affected.

IMPEDANCE INVERSION: HUSSAR WELL LOGS EXAMPLE

The real-world influence of bandlimitation on inversion can also be straightforwardly illustrated. Here we will do so with data from well 12-27 of this year's Hussar field experiment (Margrave et al., 2011). The logs permit local normal incidence P-wave reflection

*FWI requires us to take as an article of faith that iteration n knows it better than did iteration n-1.

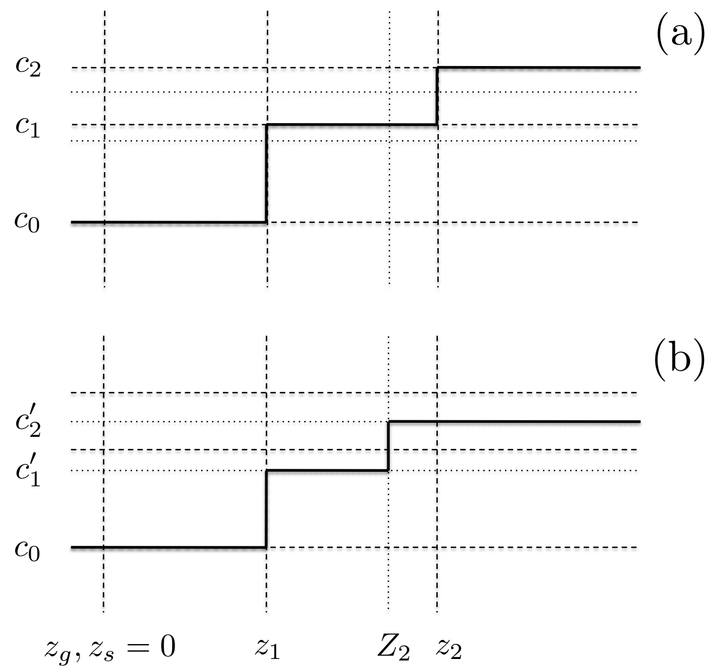

FIG. 3. True and estimated Earth models after iteration 1: (a) correct, or "actual" Earth; (b) FWI result. Two interfaces have been constructed, with error in the relative amplitudes and in the placement of any interface underlying Earth material *not* included correctly in the background model.

coefficients and velocity profile to be estimated, and these in turn used to generate the effective, full bandwidth, reflectivity series. This reflectivity series may then be subjected to P-wave impedance inversion, recovering the velocity profile as if full bandwidth data had been provided (Figure 4, black profile).

The reflectivity can be further processed to correspond to a more realistic, bandlimited, signal, with its lowest frequencies missing. We next carry this out, eliminating the lowest (A) 1 Hz, (B) 5 Hz, and (C) 10 Hz, and again subject them to impedance inversion. These are plotted in Figure 4, with (A) in blue, (B) in red and (C) in green.

It is interesting to see the same behaviour here as we noted earlier for linear inverse scattering (which turned out to be true for full waveform inversion also): the blue, red and green curves, deficient in low frequencies, cannot sustain in depth the true structure of the impedance profile (seen in black).

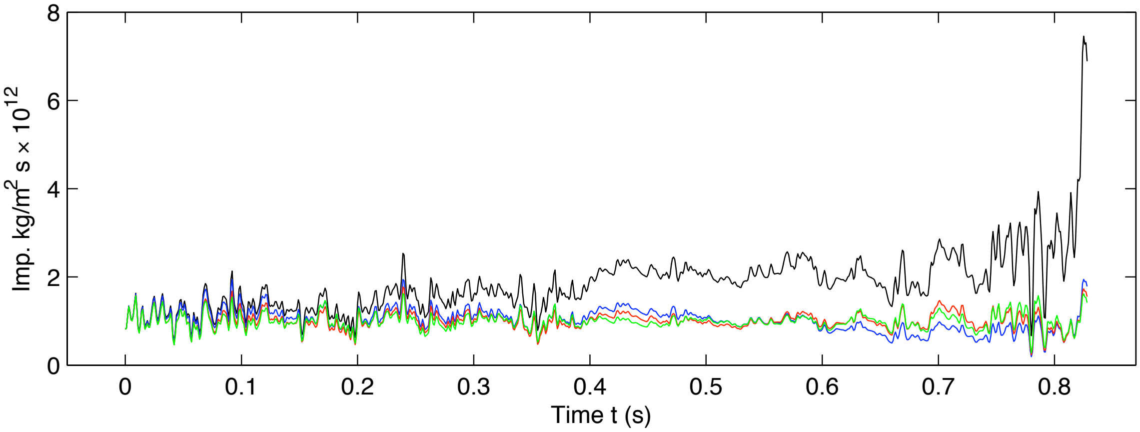

FIG. 4. Impedance inversion of reflectivity series estimated from Hussar well data at well 12-27. Black: full bandwidth; blue: lowest 1 Hz missing; red: lowest 5 Hz missing; green: lowest 10 Hz missing.

CONCLUSIONS

CREWES has made a significant effort this year to support seismic inversion by generating (1) data rich in low frequencies (the Hussar experiment), and (2) model-based methods to extend the spectra of bandlimited data. Here we provide in a tutorial setting illustrations of the reasons why missing low frequencies have such a deleterious influence on inversion. After a brief review of inverse scattering and full waveform inversion, 1D examples quickly expose the influence of low frequencies, as does an example synthesized from Hussar well-log data.

ACKNOWLEDGMENTS

The sponsors of CREWES and NSERC are gratefully acknowledged for their support.

REFERENCES

Clayton, R. W., and Stolt, R. H., 1981, A Born-WKBJ inversion method for acoustic reflection data: Geophysics, **46**, No. 11, 1559–1567.

Innanen, K. A., 2008, A direct non-linear inversion of primary wave data reflecting from extended, heterogeneous media: Inverse Problems, **24**, 035,021.

Margrave, G. F., Bertram, M. B., Lawton, D. C., Innanen, K. A., Hall, K. W., Mewhort, L., and Hall, M., 2011, The Hussar low-frequency experiment: CREWES Annual Report (this report), **23**.